The Greenland-Ice-Sheet evolution over the last 24,000 years: insights from model simulations evaluated against ice-extent markers

Tancrède P.M. Leger[1,2], Jeremy C. Ely[1], Christopher D. Clark[1], Sarah L. Bradley[1], Rosie E. Archer[3], Jiang Zhu[4]

[1] School of Geography and Planning, University of Sheffield, Sheffield, S10 2TN, UK

[2] Institute of Earth Surface Dynamics, University of Lausanne, Lausanne, Switzerland

[3] Department of Geography and Environmental Sciences, Northumbria University, Newcastle, UK

[4] Climate and Global Dynamics Laboratory, NSF National Center for Atmospheric Research, Boulder, CO, USA

Supplementary materials

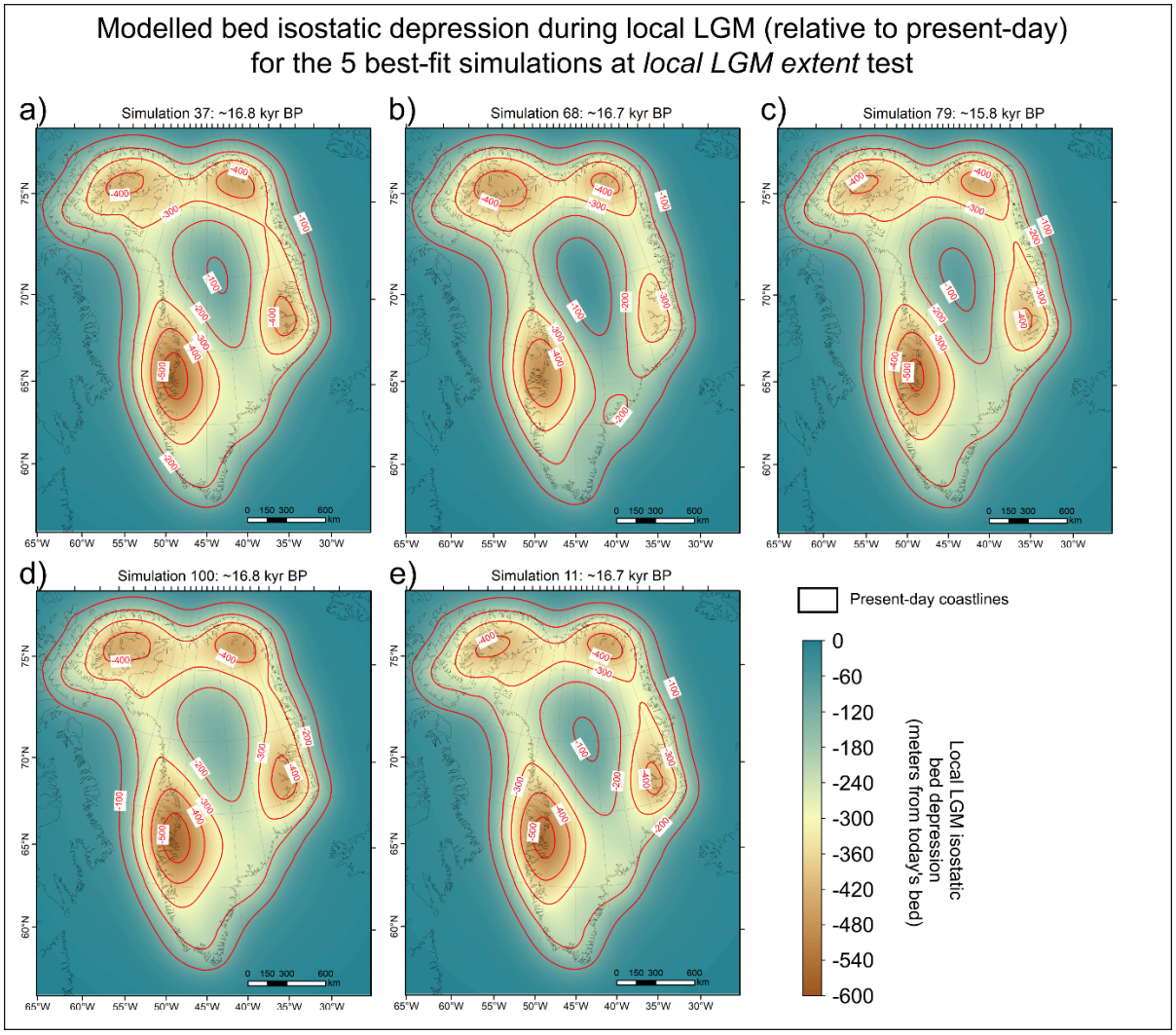

Supplementary figure 1. Modelled bed isostatic depression during the local LGM (timing is simulation-dependent), relative to the present-day bed topography, for the 5 best-scoring ensemble simulations at the *local LGM extent* test.

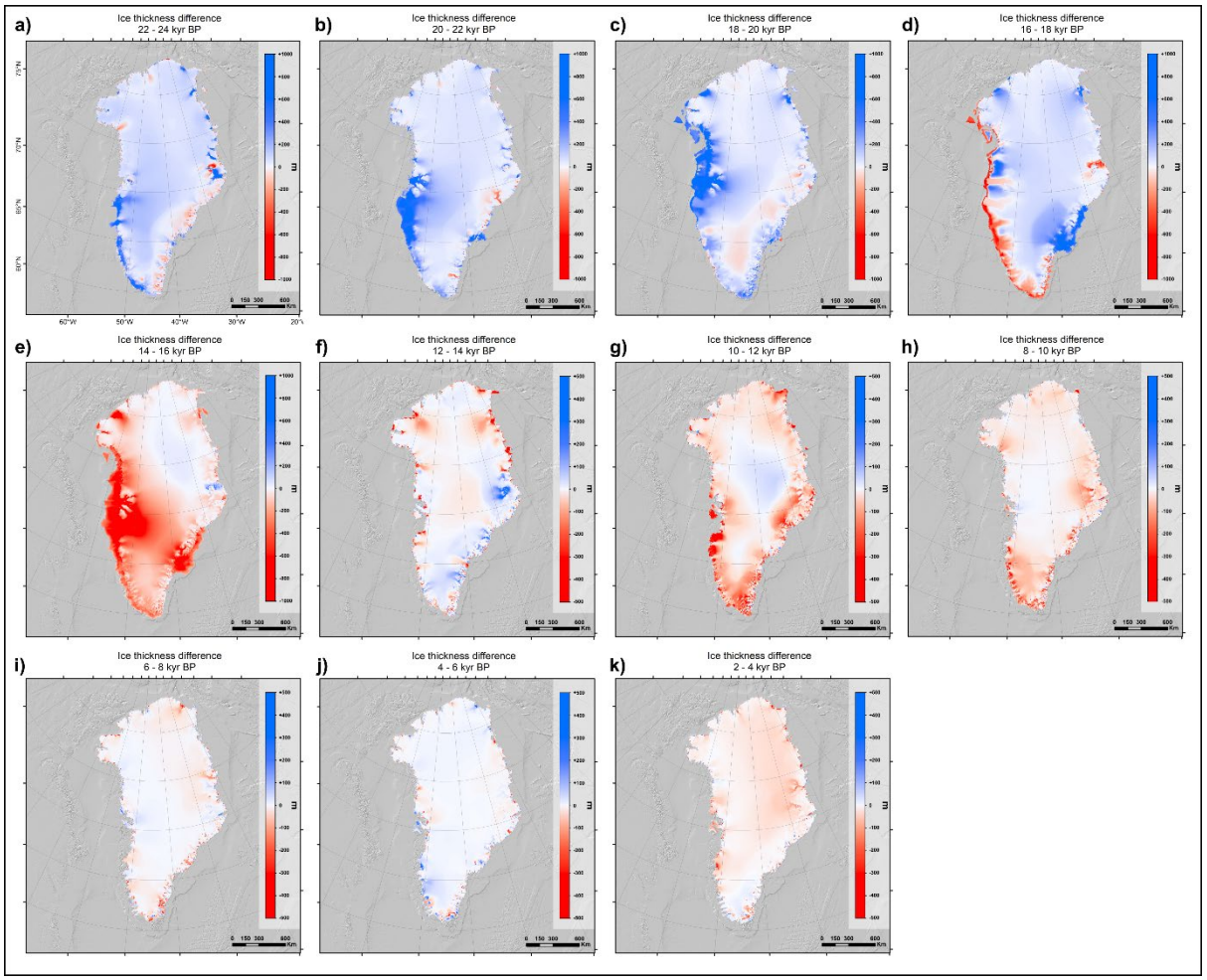

Supplementary figure 2. 2 kyr ice thickness difference maps between 24 - 22 and 4 - 2 kyr BP for one of the 5 overall best-fit simulations (which passes all sieves); simulation number 26. Note that the ice-thickness-difference colorbar minimum and maximum values are different between panels a - e (range: +1000 ; -1000), and panels f - k (range: +500 ; -500).

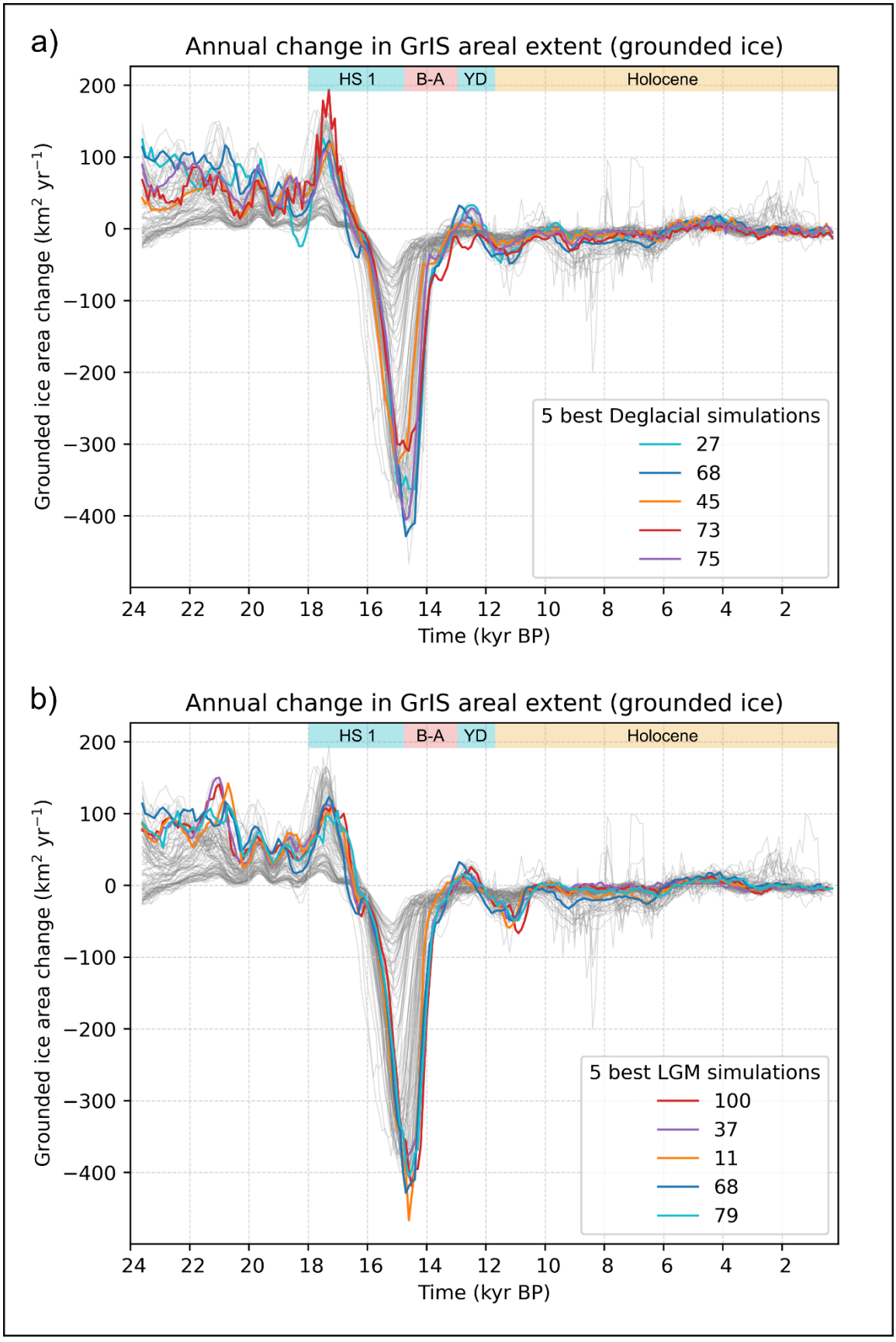

Supplementary figure 3. Ensemble time series (thin grey lines) of modelled annual change in GrIS-wide grounded ice areal extent, with best-scoring simulations at both the *deglacial extent* test (panel a) and the *local-LGM extent* test (panel b) highlighted with thick coloured time series.

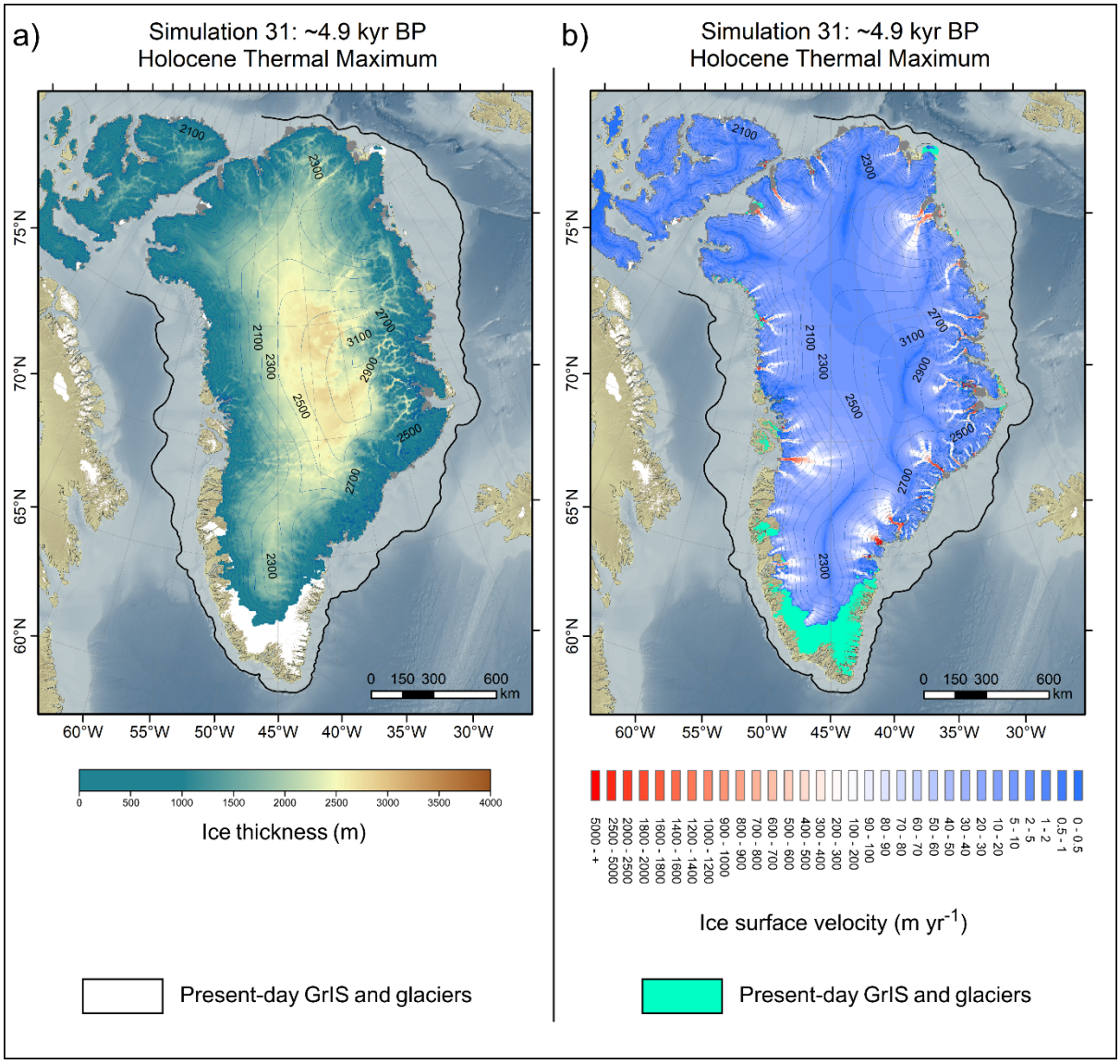

Supplementary figure 4. Modelled ice thickness (panel a) and ice-surface velocities (panel b) at approximately 5 kyr BP, during minimum Holocene ice extent, for the best-scoring ensemble simulation at the PI-extent test, *i.e.* simulation 31. This figure highlights the magnitude of retreat of modelled GrIS margins following the Holocene Thermal Maximum, in some regions reaching behind the present-day GrIS margin (in white (panel a) or bright green (panel b)). On both panels, contour lines are 200 m ice-surface elevation contour intervals.

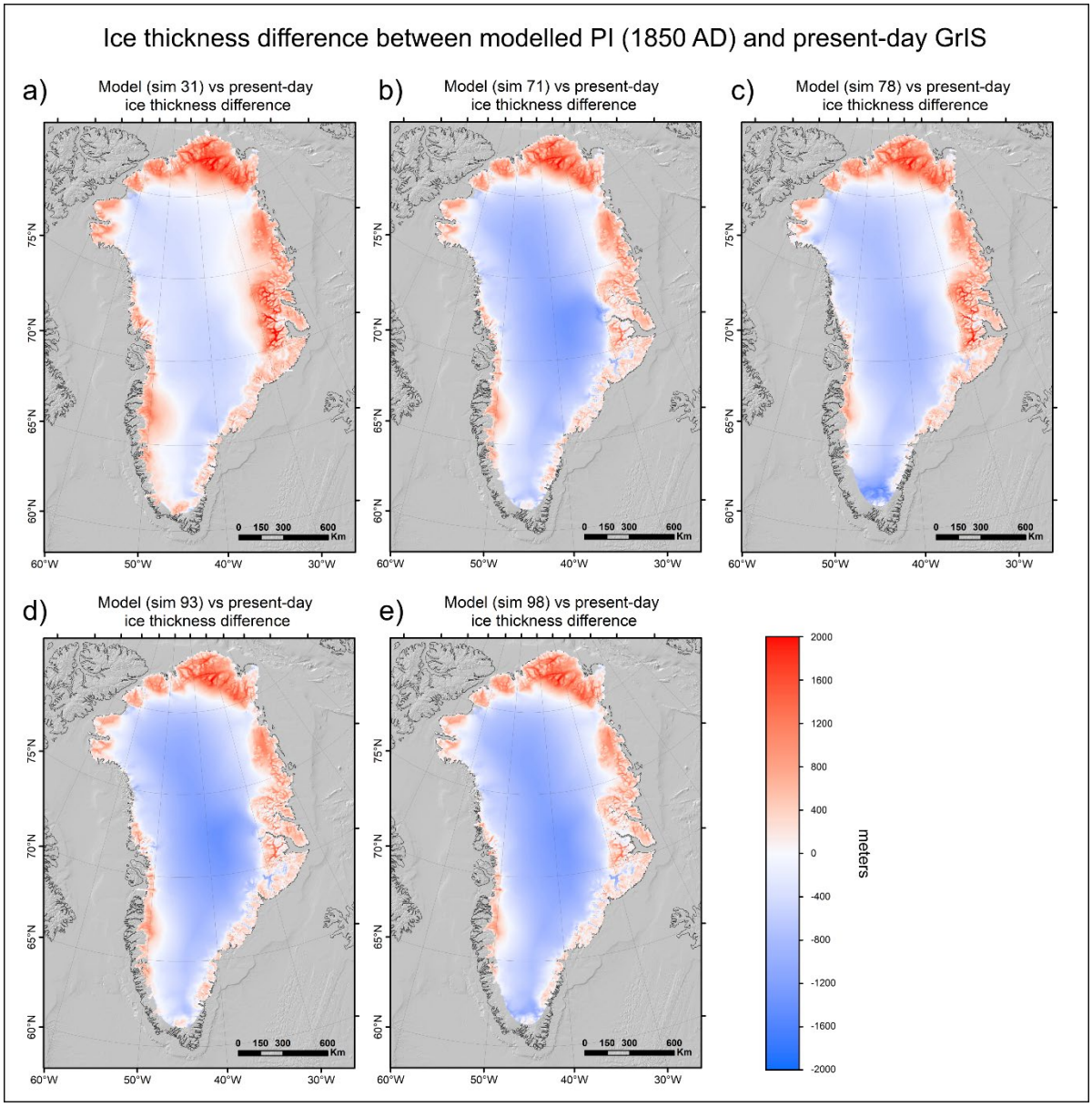

Supplementary figure 5. GrIS thickness difference between modelled PI states (1850 AD) versus the reconstructed present-day GrIS ice thickness (BedMachine v4: Morlighem et al., 2017) for the 5 best-scoring simulations at the *PI extent* test.

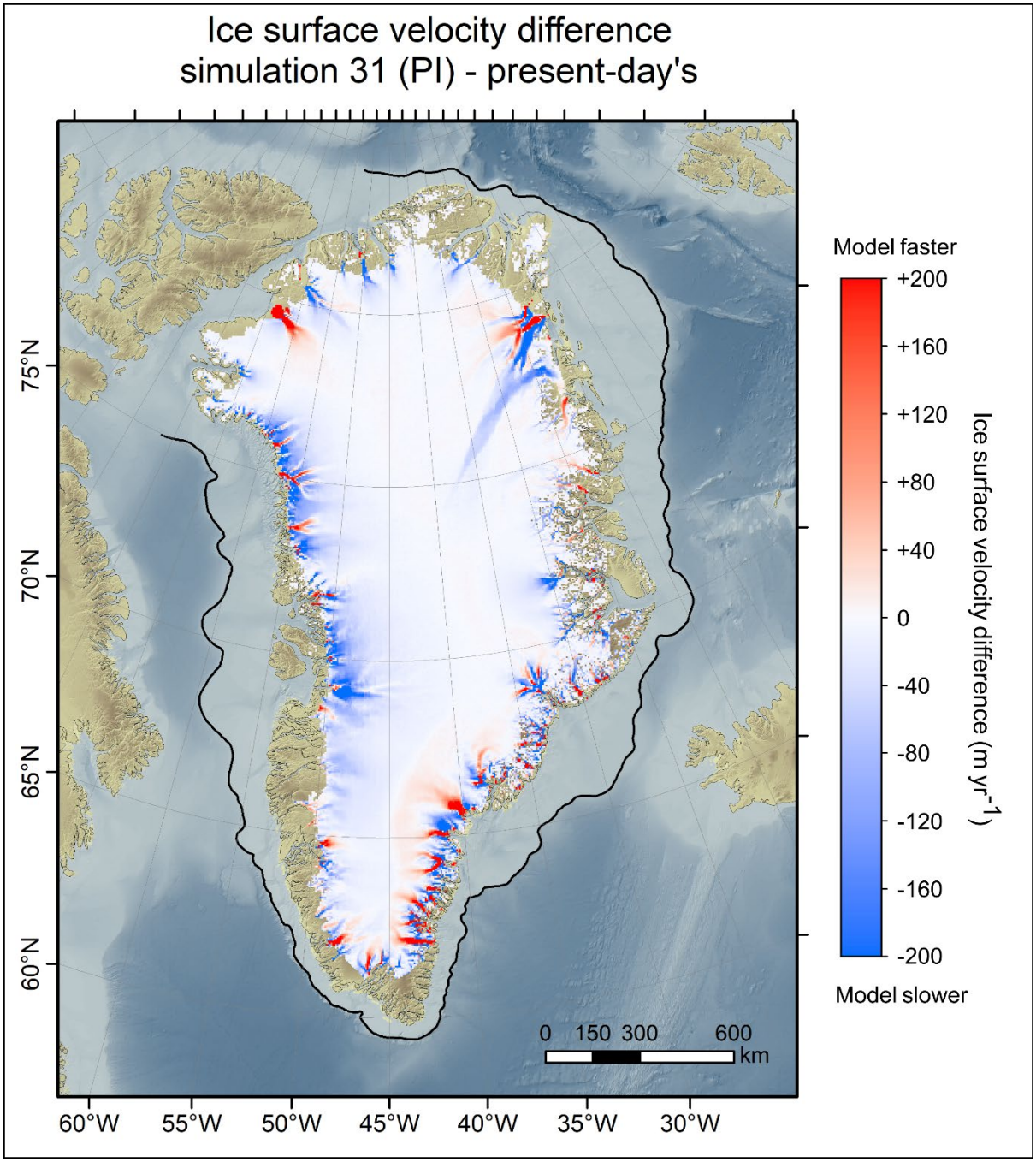

Supplementary figure 6. Modelled ice-surface velocity difference between modelled PI state (1850 AD) for the best-scoring simulation at the PI extent test (i.e. simulation 31) versus observed present-day ice surface velocities of the GrIS (Joughin et al. 2018).

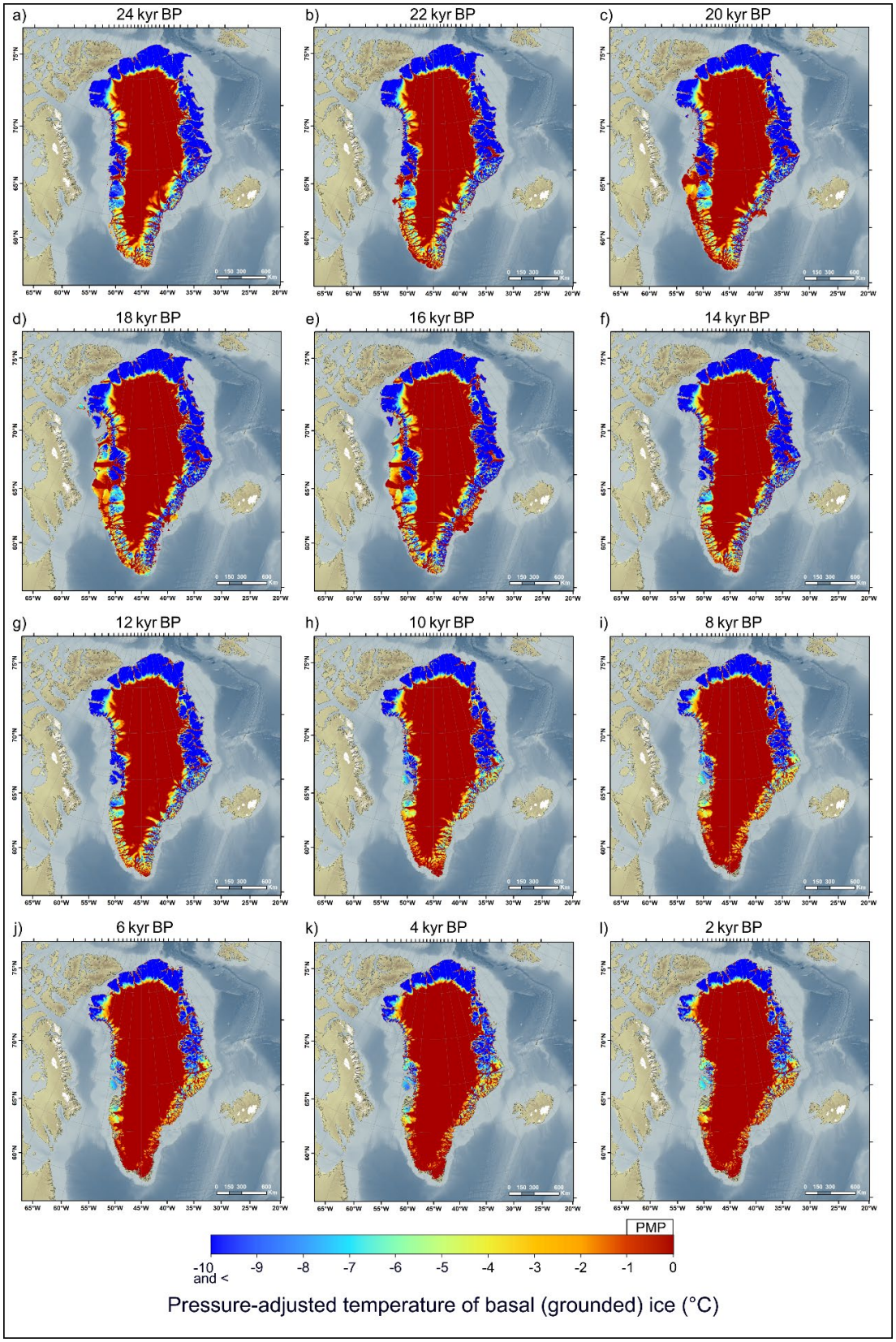

Supplementary figure 7. Pressure-adjusted modelled basal ice temperature of grounded ice for one of our ensemble's overall best-fit simulations (which passes all sieves: simulation number 26). The model output data is shown for timeslices every 2 kyr, between 24 and 2 kyr BP. 'PMP' stands for 'pressure-melting point'.

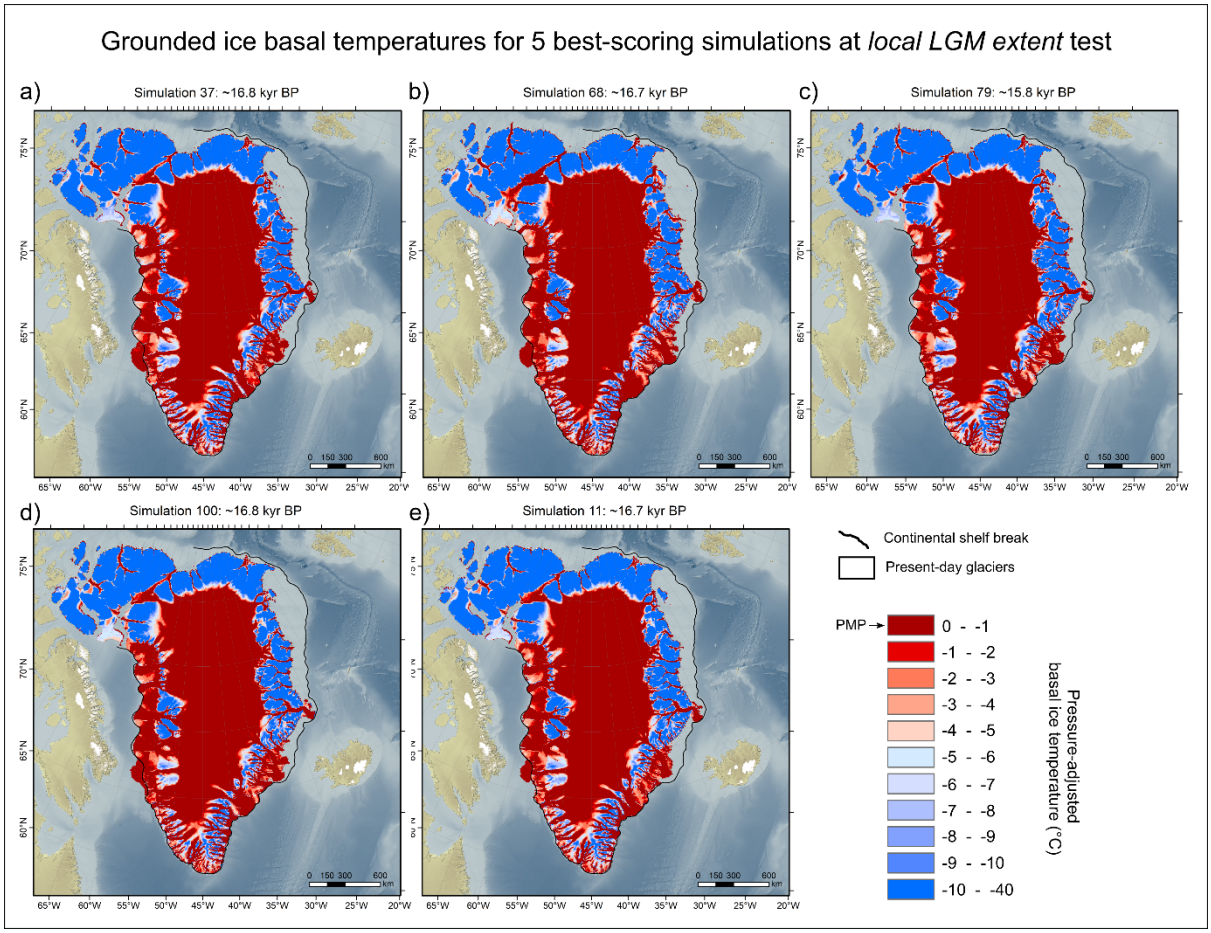

Supplementary figure 8. Modelled basal ice temperatures for grounded ice during the local LGM (timing is simulation-dependent) for the 5 best-scoring ensemble simulations at the *local LGM extent* test. 'PMP' stands for 'pressure-melting point'.

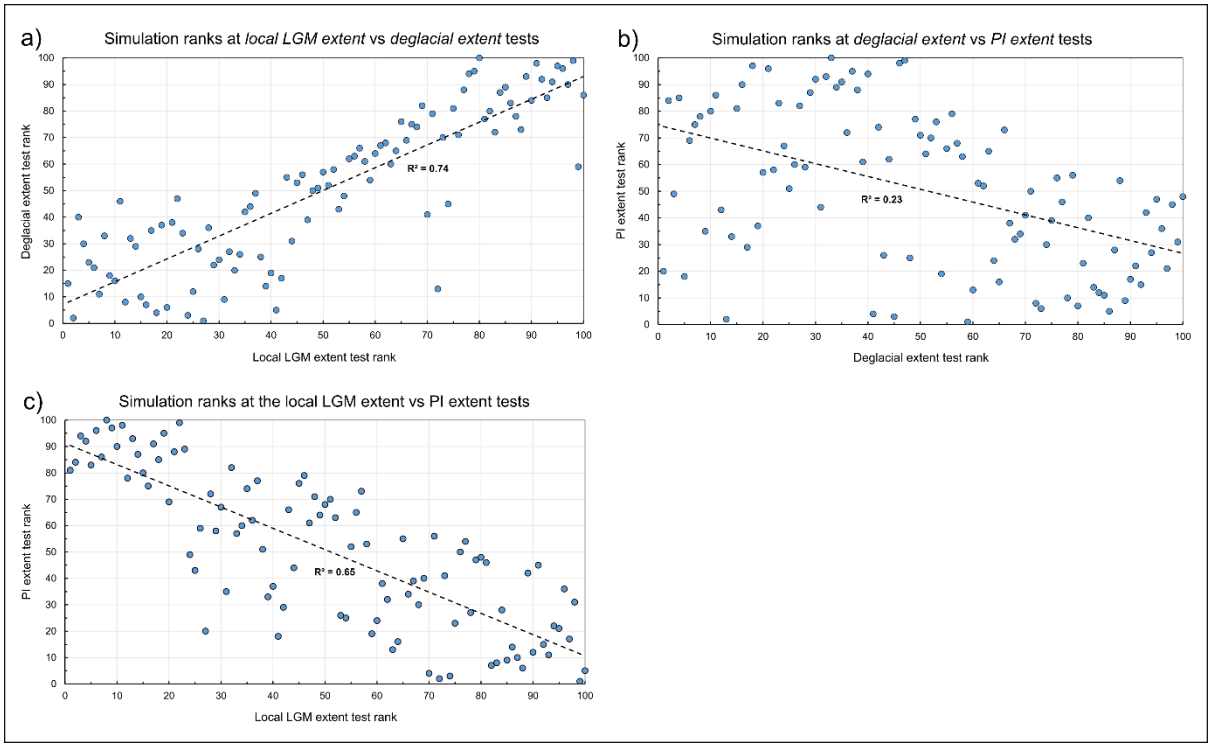

Supplementary figure 9. Linear regressions between ensemble simulation relative ranks at one of our three model-data comparison tests (*e.g. PI extent* test) versus another. A high rank (e.g. 1) is equivalent to the best-scoring simulation, while a low rank (e.g. 100) represents the worse-scoring simulation. Ensemble simulations that score well at the *local LGM extent* test also tend to score well at the *deglacial extent* test ($R^2 = 0.74$) (panel a), for instance, while a negative correlation ($R^2 = 0.65$) can be observed between *local LGM extent* test ranks and PI extent test ranks (panel c).

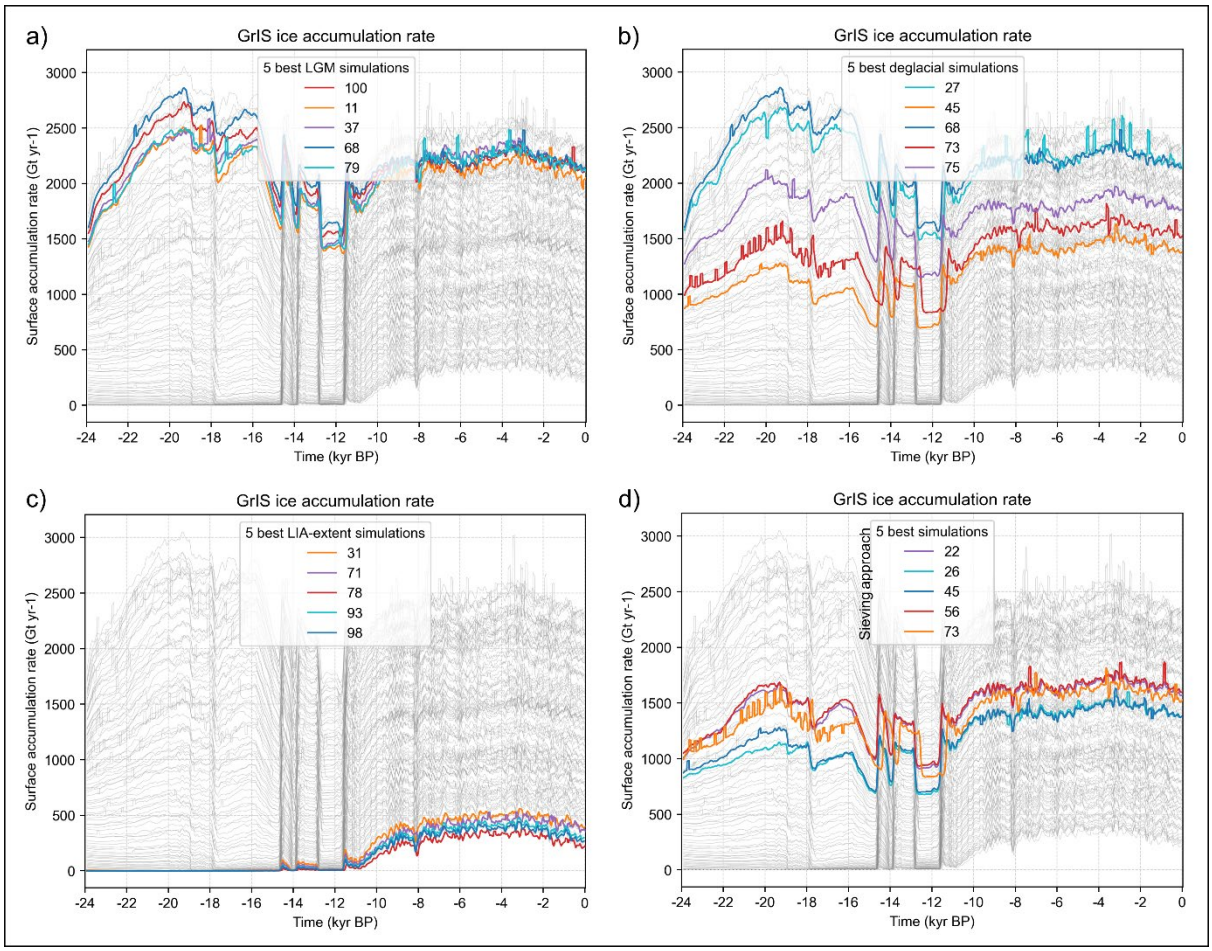

Supplementary figure 10: Ensemble time series of modelled GrIS-wide integrated ice accumulation rate. The best-scoring simulations at each of our three model-data comparison tests (panels a – c), and for the five overall best-fit simulations (which pass all sieves; panel d) highlighted in thick coloured time series.

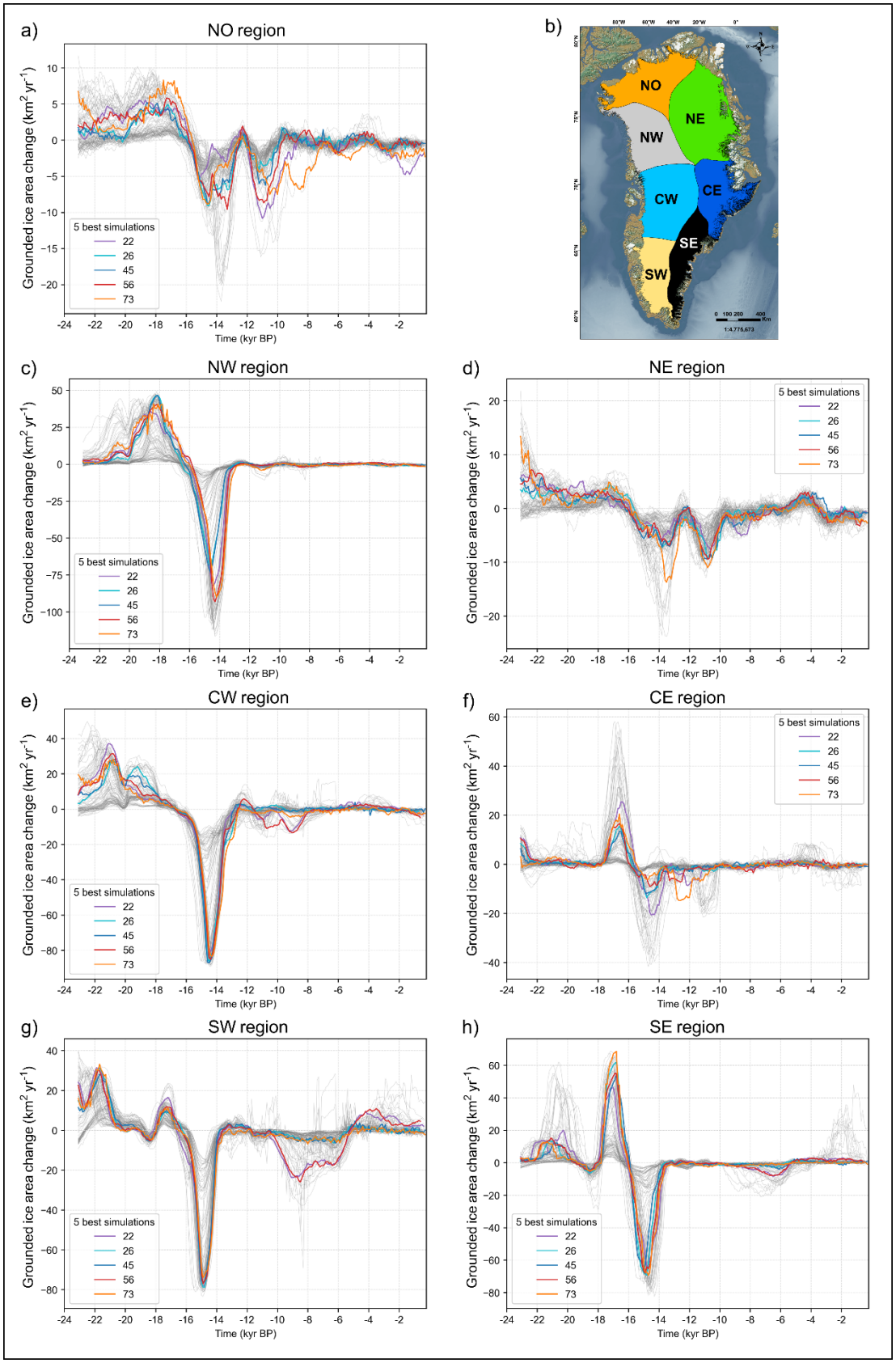

Supplementary figure 11: Ensemble time series (thin grey lines) of modelled annual change in GrIS-wide grounded ice area for each of the seven main GrIS regions (whose location are shown in panel b). The 5 overall best-fit simulations (which pass all sieves) are highlighted with thick coloured times series.

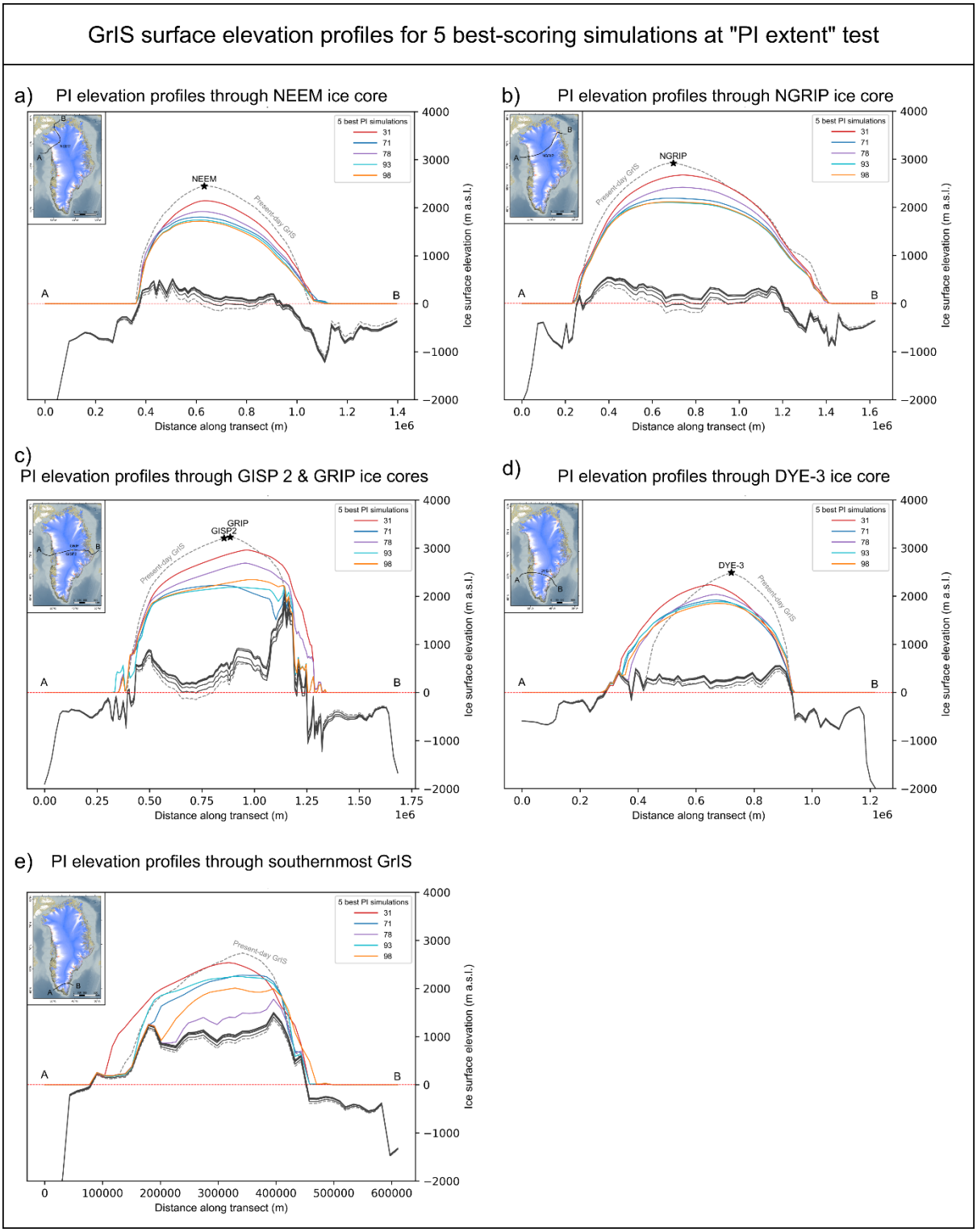

Supplementary figure 12: Modelled ice surface and bed elevations during the PI (1850 AD) extracted across five different transects for our five best-scoring simulations at the *PI extent* test (thicker coloured lines), and for the present-day GrIS (dashed grey lines). The four transects were drawn following modelled ice flow lines while ensuring to cross the NEEM (panel a), NGRIP (panel b), GISP 2 and GRIP (panel c), and the DYE-3 (panel d) ice core locations, as shown by the black lines in the inset maps. The transect drawn through the southernmost GrIS (panel e) was not drawn to cross any specific ice core locations, however.

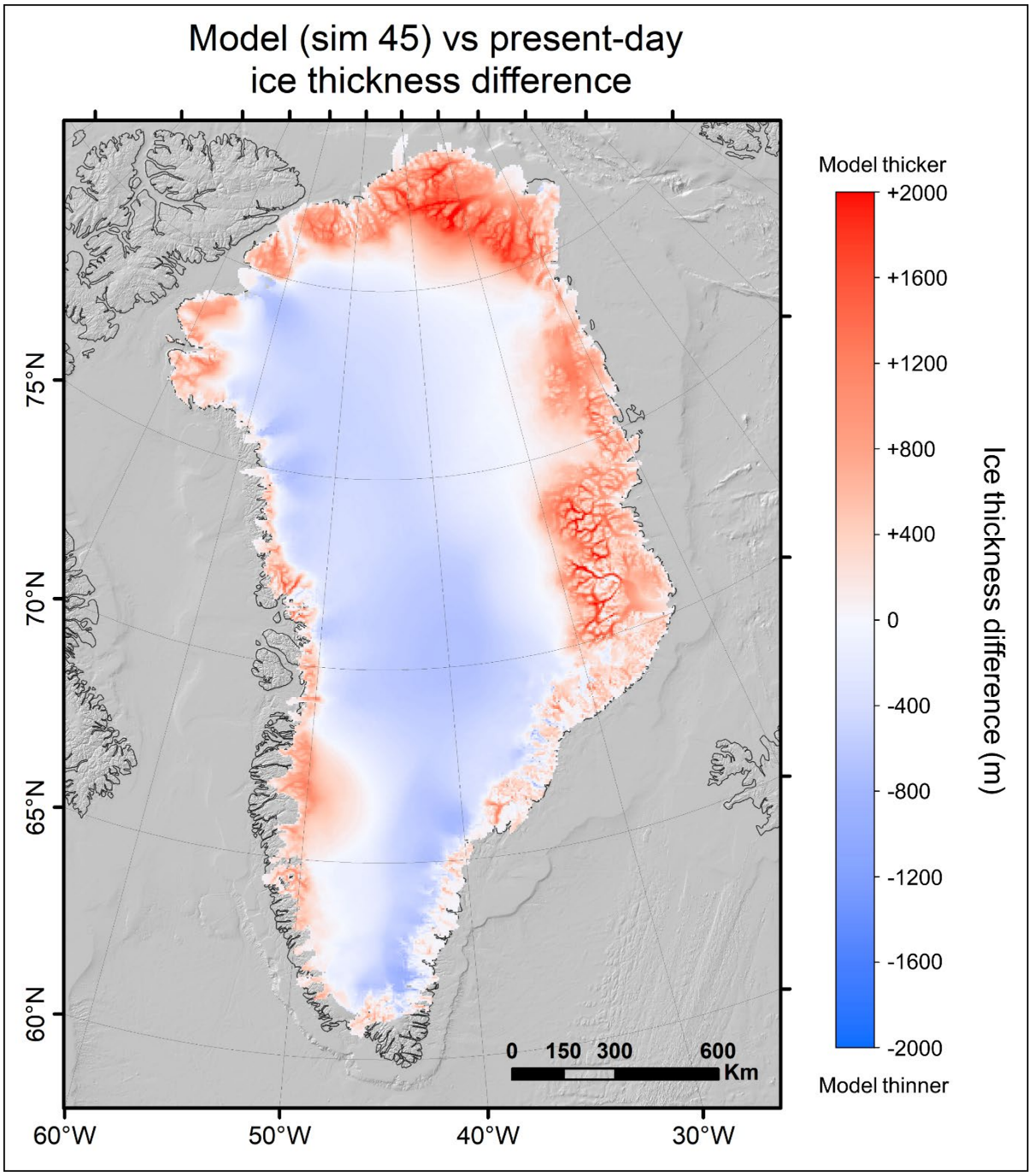

Supplementary figure 13: GrIS thickness difference between modelled PI states versus the reconstructed present-day GrIS ice thickness (BedMachine v4) for one of the 5 overall best-fit ensemble simulations (which passes all sieves), *i.e.* simulation 45.